Stress–Strain Curve Modeling and Length Effect of Polymer Concrete Subjected to Flexural Compressive Stress

Kyu-Seok Yeon

Department of Regional Infrastructures Engineering, Regional Infrastructures Engineering Program, Kangwon National University, Chuncheon 200-701, Korea

Received 12 September 2008; accepted 23 June 2009
DOI 10.1002/app.30992
Published online 17 August 2009 in Wiley InterScience (www.interscience.wiley.com).

ABSTRACT: Stress–strain relation, stress-block parameters, and length effect of polymer concrete flexural compression members were experimentally investigated. For these purposes, a series of C-shaped polymer concrete specimens subjected to a flexural compressive load were tested. On the basis of the test results, we proposed an equation to predict stress–strain relation of polymer concrete. In this model, we took account of the slope of descending branch beyond the peak stress point of a single curve. The proposed equation was numerically integrated to compute the rectangular stress-block parameters. Computed β_1 was greater than the values prescribed in ACI 318 Code for cement concrete, and α_1 was about 0.85 that is similar to the value regulated in ACI. A series of C-shaped specimens were also tested to study the length effect. The test results were curve fitted to obtain parameters for the existing length effect equation. © 2009 Wiley Periodicals, Inc. J Appl Polym Sci 114: 3819–3826, 2009

Key words: mechanical properties; modeling; stress; strain

INTRODUCTION

Cement concrete is widely used as construction material even if it has the problem of low strength that gives rise to heavyweight and large cross-section. To solve these problems, high-strength and lightweight construction materials need to be used. One of these materials suggested for this purpose is polymer concrete. Conventional cement concrete has low tensile and flexural strengths that easily cause cracks, and it has low chemical resistance as well. On the other hand, the polymer concrete has high compressive, tensile and flexural strengths, as well as superior physical and chemical properties such as a short curing time, impact resistance, chemical resistance, electrical insulation, waterproofness, and freeze–thaw durability. Furthermore, the polymer concrete has been widely used as a structural material because it has not only good adhesion to other materials such as reinforcing rods and cement concrete, but also good resistance to impact water and corrosion. That is, the polymer concrete is rather a new construction material that can be used for repairing concrete structures as well as for beams and slabs of thin cross sections, precast manholes, electric culverts, sleepers, and dry walling for buildings.[1–4]

To widen the applicability of polymer concrete, researches on its structural properties should be carried out and design standards should be prepared. However, very limited number of studies about structural behavior of the polymer concrete has been conducted, and application standards for it are not established. To make the design standard, extensive data for structural behavior of the polymer concrete are necessary.

In general, the strength and stress–strain relation of polymer concrete depend on curing and field temperatures.[5] Because the polymer concrete shows a brittle fracture, improving its postpeak stress–strain behavior is important. It is therefore essential to the polymer concrete applications to develop better structures and to understand the characteristics of compressive strength corresponding to constituents. Methyl methacrylate (MMA) can be added to polymer concrete using unsaturated polyester (UP) resin to improve its workability. Especially, in material aspect, more researches are necessary to survey the stress–strain relation required in designing the polymer concrete structures. However, fundamental data about stress–strain relationship of polymer concretes are not sufficient enough.[6,7]

Because brittle materials are usually fractured due to occurring cracks, size effect has to be implemented. The size effect is quite apparent in the compressive fracture of the brittle materials.[8] The

Correspondence to: K.-S. Yeon (ksyeon@kangwon.ac.kr).
Contract grant sponsor: Korea Institute of Construction & Transportation Technology Evaluation and Planning (KICTTEP), (Ministry of Construction and Transportation).

TABLE I
Physical Properties of Materials for Binder System

Unsaturated polyester resin			
Density (g/cm^3, 20°C)	Viscosity (mPa s, 20°C)	Acid value	Styrene content (%)
1.13	300	20.0	40.0
Methyl methacrylate			
Density (g/cm^3, 20°C)	Viscosity (mPa s, 20°C)	Molecular weight (g/mol)	Appearance
0.94	0.56	100	Transparent
Shrinkage-reducing agent			
Density (g/cm^3, 20°C)	Viscosity (mPa s, 20°C)	Nonvolatile content (%)	Appearance
1.11	3100–4100	34–38	Transparent

researches of the compressive fracture behavior have been extensively carried out, but those of the mechanism of compressive fracture are not sufficient compared with those of tensile fracture. In the case of concretes, many researches showed that compressive strength decreases as specimen size increases, but the systematic researches on the size effect of polymer concretes are not enough yet.

In this study, the stress–strain relation and the stress-block parameters of the flexural compression member of a polymer concrete are experimentally investigated by testing a series of C-shaped specimens subjected to axial compressive load. The C-shaped specimens are also tested to study the length effect.

EXPERIMENTAL

Materials

Liquid type orthophthalate-type UP resin and MMA were used as binder. Forty-five percent dimethyl phthalate solution of methyl ethyl ketone peroxide was used as an initiator, and 6% solution of cobalt octoate (CoOc) was done as a promoter. To reduce the setting shrinkage, shrinkage-reducing agent (SRA) made by dissolving polystyrene into styrene monomer was used.

The contents of UP and MMA in mass fraction of the liquid resin were 70% and 30%, respectively. SRA content was 15% out of UP content. The binder system contained 0.75% of initiator and 0.50% of promoter. The physical properties of the materials for a binder system are shown in Table I.

Commercially available ground calcium carbonate (size of 13 μm in average) was used as filler. Crushed stone (size of 5.0–13.0 mm) from limestone was used as a coarse aggregate, crushed sand (C) (size of 0.8–5.0 mm), and crushed sand (F) (size of 0.0–0.8 mm) from limestone were used as fine aggregates. The properties of filler and aggregates are shown in Table II.

Flexural compressive test for C-shaped specimen

To determine the characteristic compressive properties of polymer concrete formulation, standard cylindrical specimens measuring 50 mm of diameter and 100 mm of length were previously tested in compression according to JIS A 1181.[9] Average values of 100 MPa, 22,000 MPa, and 2.2 were found for compressive strength, compressive elastic modulus, and Poisson ratio, respectively. The mix proportion for making the specimens is shown in Table III.

Specimen

The dimensions, shape, and loading point locations of C-shaped specimens used in this study are shown in Figure 1. The mid-height of C-shaped specimens, which is the critical section under compression is not reinforced. The flexural and shear reinforcements are inserted at both ends of the specimen to eliminate the undesired premature shear failure at the two end sections and ensure failure in the mid-height of the specimen. The circular pole of 3 cm diameter was inserted at the end of specimen to install a steel rod to which an eccentric load is applied. The thickness and the

TABLE II
Physical Properties of Filler and Fine Aggregates

Type of filler or aggregate	Size (mm)	Real density (g/cm^3, 20°C)	Water content (%)	Organic impurities
Ground calcium carbonate	13×10^{-3}	2.73	<0.1	Nil
Coarse aggregate	5.0–13.0	2.78	<0.1	Nil
Fine aggregate (C)	0.8–5.0	2.62	<0.1	Nil
Fine aggregate (F)	0.0–0.8	2.45	<0.1	Nil

TABLE III
Mix Proportion for Polymer Concrete

Mix proportions (%) (mass fraction)						
Binder	Filler	Coarse aggregate	Fine aggregate (C)	Fine aggregate (F)	Binder content (%) (mass fraction)	Binder to filler ratio (mass fraction)
UP-MMA system	Ground calcium carbonate	Crushed stone	Crushed sand	Crushed sand		
8.5	17.0	44.7	14.9	14.9	8.5	1.0 : 2.0

depth of all specimens are kept constants; the thickness is 12.5 cm and the depth is 10 cm. A total of 12 specimens were prepared with four different lengths: 10, 20, 30, and 40 cm (three specimens for each length). Figure 2 shows photo of test setup.

Test method

For experiments on concrete beams subjected to flexural loads, the size and the length or depth effect cannot be evaluated systematically because of the change in the location of the neutral axis of the cross section as member sizes, reinforcement ratios, applied loading increments, loading point locations, etc. vary.[10] To resolve these problems, C-shaped concrete specimens subjected to axial load and bending moment can be used.[10] The position of the neutral axis is kept fixed by continuously monitoring strains on one surface of the C-shaped specimen and adjusting the eccentricity of the applied force so that the depth of neutral surface remains the same.[8]

A total of 12 strain gauges were attached on the compressive face, the tension face, and the lateral face of specimen: four strain gauges were installed at each face. Also, two LVDTs were installed at the compressive face to measure the relative deflection of mid-height of specimen when compared with that of the end. The data obtained from the LVDT were averaged to get average displacement and used to adjust the load lever arm (a_1 and a_2) that was used to calculate flexural moment.

The load applying procedure is as follows:

i. Load P_1 is applied until the strain gauge on the tension face reads a specific value (100×10^{-6} mm/mm).
ii. Eccentric load P_2 is incrementally applied until the strain value of tension face reaches zero.
iii. When the average of strain values reaches zero, the load P_2 is maintained while P_1 is further increased.
iv. This procedure is repeated until the specimen fails.

RESULTS AND DISCUSSION

Depth-strain relation

Figure 3(a) depicts the lateral face strain measurement at six strain gauge positions for 10 different loading stages, $P_u/10$, $2P_u/10$, . . ., and P_u (P_u: ultimate load),

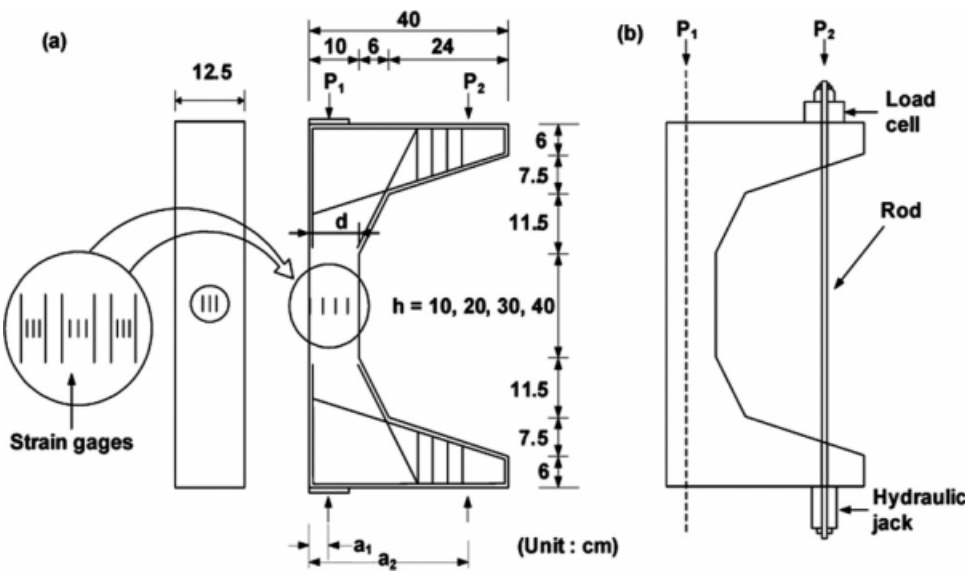

Figure 1 (a) Shape and size, and (b) loading equipment of C-shaped specimen.

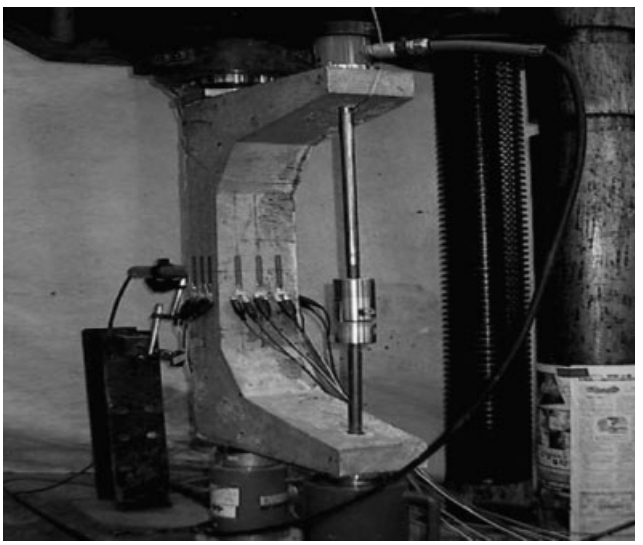

Figure 2 Photo of test setup.

for the specimen with $h/d = 1$ [Fig. 3(b) shows the positions of strain gauges]. As shown in the figure, the strains for each loading stage vary closely linearly. The graph proves that plane sections remain plane after deformation is valid for C-shaped specimen of polymer concrete, that is, the neural axis remains at the position of 0 depth during the test.

Compressive stress–strain model

Stress–strain relation is affected by several factors and defining just one valid model for each polymer concrete is impossible. However, the stress–strain relation to predict polymer concrete behaviors is necessary. In the case of ordinary concrete, for example, numerous models are proposed by several authors. Some of these are Hognestad et al.,[11] Kent and Park,[12] Sheik and Uzumeri,[13] Roy and Sozen,[14] Sargin,[15] Saatcioglu and Razvi,[16] Muguruma et al.,[17] Collins et al.,[18] and Hsu and Hsu.[19]

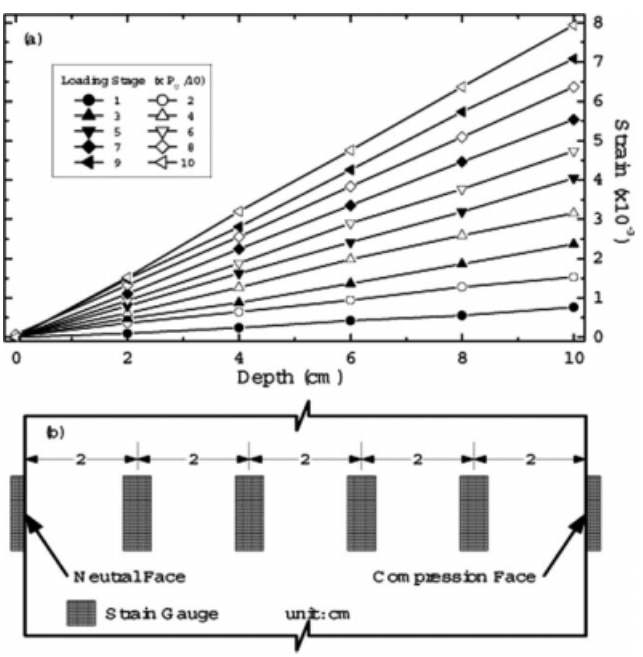

Figure 3 (a) Depth-strain relations on six different depths for $h/d = 1$ (P_u: ultimate load), (b) positions of strain gauges.

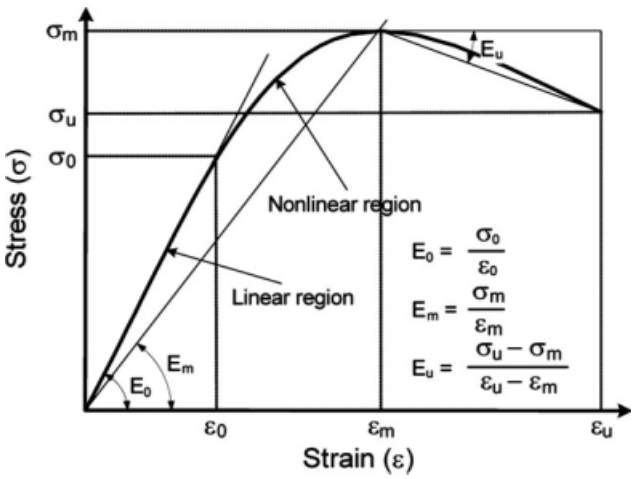

Figure 4 Typical monotonic stress–strain relation of compression and notations used in this study.

For the ordinary-, high-, and ultra high-strength concretes, the analyses and behaviors of structures largely depend on the form of stress–strain model. In the same manner, the model equation for polymer concrete should be definitely represented to compute the equivalent stress-block parameters exactly.

Two methods are usually used to represent the stress–strain curves; one method is to express the ascending and the descending branches separately, and another method is to express both branches in a single curve. Representative single curve model was suggested by Sargin and Handa[20] as eq. (1).

$$Y = \frac{AX + (B-1)X^2}{1 + (A-2)X + BX^2}, \tag{1}$$

where, $X = \varepsilon/\varepsilon_m$, $Y = \sigma/\sigma_m$ (or $= f_c/f'_c$), σ is the stress of specimen (N/mm^2), σ_m is the maximum stress (N/mm^2), ε is strain and ε_m is the strain at σ_m,

TABLE IV
Proposed Definitions of A and B by Several Authors

Authors	A	B	Note
Sargin and Handa[20]	E_0/E_m	0	$f'_c \geq 50$ N/mm^2
Ahmad and Shah[21]	E_0/E_m	0.876A–0.8164	
Sun and Sakino[22]	E_0/E_m	1.5–0.00168 f'_c	
Saenz[23]	E_0/E_m	1	

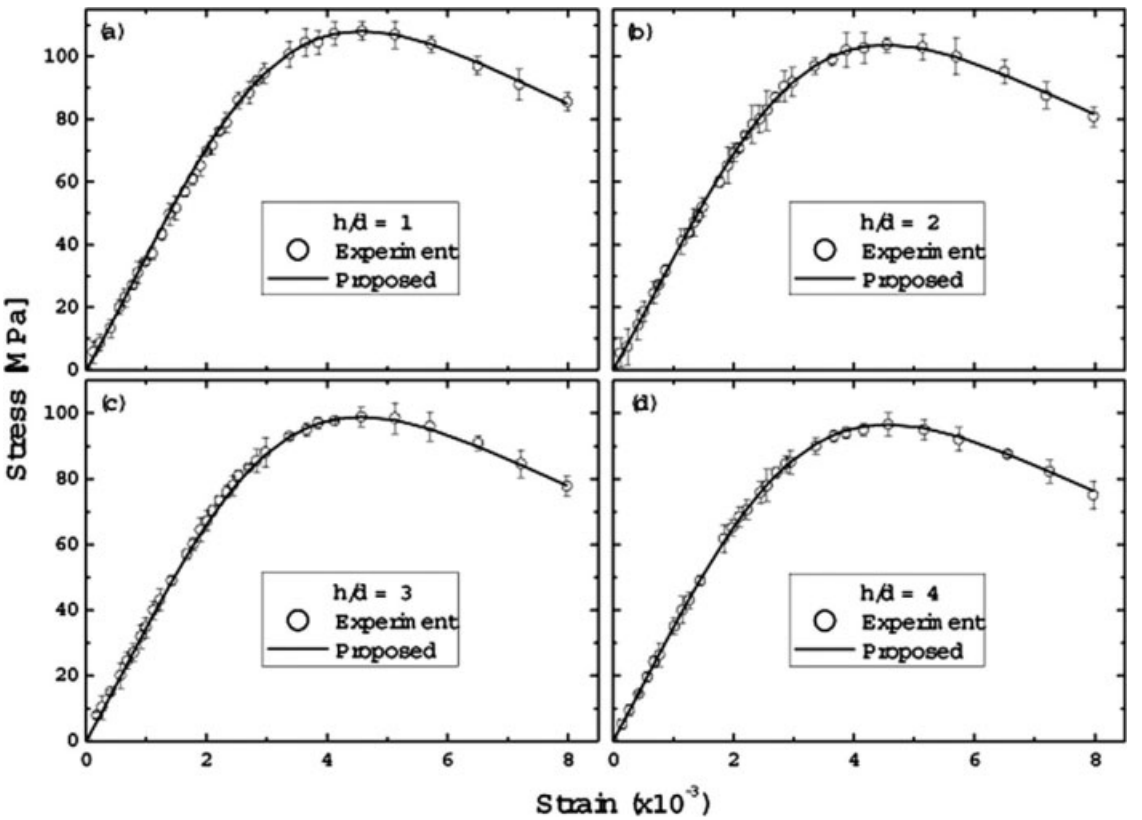

Figure 5 Plots of experimental results and proposed stress–strain model for polymer concrete.

f_c is the compressive strength, and f'_c is the standard compressive strength of cylinder specimen. Authors are free to choose the constants or formulae A and B according to their study.

Figure 4 depicts the schematic single compressive stress–strain curve and shows the notations used in this study. Many authors, for example, Sargin and Handa,[20] Ahmad and Shah,[21] Sun and Sakino,[22] and Saenz[23] suggested the stress–strain relation for concrete specimens with different forms of A and B. Table IV lists A and B suggested by the authors.

We proposed the stress–strain relation of a single curve for the C-shaped polymer concrete structures studied in this article as eq. (2) by using eq. (1) as a basic equation.

$$\sigma(\varepsilon) = \sigma_m \frac{E_r X + (E_u - 1)X^2}{1 + (E_r - 2)X + E_u X^2}, \qquad (2)$$

where $E_r = E_0/E_m$, $E_0 = \sigma_0/\varepsilon_0$ (initial elastic modulus), $E_m = \sigma_m/\varepsilon_m$, $E_u = (\sigma_u - \sigma_m)/(\varepsilon_u - \varepsilon_m)$ (the average slope of descending branch), σ_u is the ultimate stress and ε_u is the ultimate strain. It is noted that the factor of E_u controls the steepness rate for the descending branch beyond the peak stress point of the stress–strain relation.

Figure 5 shows the experimental results and the proposed stress–strain models for four different length to depth ratios r (=h/d) of C-shaped polymer concrete specimens. As shown in the figures, the suggested model is well fitted to the experimental results. In eq. (2), parameters that determine the shape of the curve can be trivially obtained from the test results. The initial elastic modulus E_0, however, was determined by inspecting the test data. In Figure 6, when the standard compressive strength is 108 MPa, the compressive stress–strain models

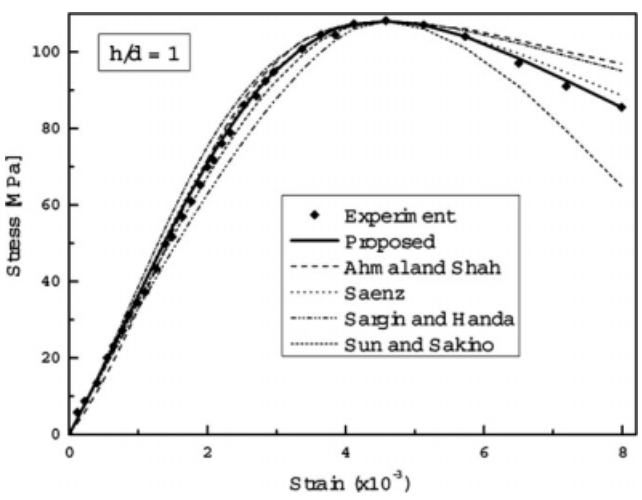

Figure 6 Comparison of models proposed by several authors.

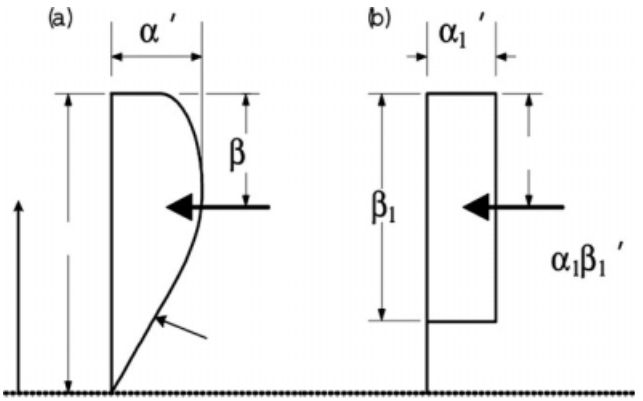

Figure 7 Analysis of rectangular stress block: (a) Actual stress distribution at ultimate state and (b) equivalent rectangle block.

proposed by aforementioned authors for ordinary concretes are compared with the experimental results and the proposed model of this study.

Equivalent rectangular stress-block parameters

Parabola, triangular, rectangular, and trapezoid distributions are generally used for the hypothesis of the flexural compressive stress distribution of concrete members. Regardless of the forms of stress blocks, the theoretical analysis about the equivalent stress blocks of concrete members is, however, possible if the compressive force C and its location of action line can be specified.

For the case of the flexural compressive members, the compressive force C and its locations of action line can be obtained by the flexural compressive test for C-shaped specimen proposed by Hognestad et al.[11] In this study, the rectangular stress-block parameters of α_1 and β_1 proposed by Whitney,[24] Figure 7, were surveyed by using the proposed equation of stress–strain relation and testing four sets of C-shaped specimens for polymer concretes.

Replacing actual stress distribution with a rectangular stress distribution requires following two conditions of eqs. (3) and (4).

i. The magnitude of resultant compressive force C should be maintained,

$$C = \int_0^c f_c(y) b \, dy = \alpha_1 \beta_1 f'_c bc = \alpha_1 f'_c ab \tag{3}$$

ii. The location of resultant compressive force C should be maintained.

$$\frac{\beta_1}{2} c = \frac{a}{2} = c - \frac{\int_0^c f_c(y) y b dy}{\int_0^c f_c(y) b dy} \tag{4}$$

where, $f_c(y)$ is the function representing the actual stress distribution, f'_c is the standard compressive strength of polymer concrete measured with cylindrical specimens, α_1 is the equivalent rectangular stress intensity coefficient, β_1 is the resultant location coefficient for an equivalent stress block, and b is the thickness of specimen. To compute the parameters using the stress–strain relation of eq. (2), eqs. (3) and (4) should be rewritten as eqs. (5) and (6), respectively:

$$C = \int_0^{\varepsilon_u} \sigma(\varepsilon) d\varepsilon = \alpha_1 f'_c a \tag{5}$$

$$\frac{\beta_1}{2} \varepsilon_u = \frac{a}{2} = \varepsilon_u - \frac{\int_0^{\varepsilon_u} \sigma(\varepsilon) \varepsilon \, d\varepsilon}{\int_0^{\varepsilon_u} \sigma(\varepsilon) \, d\varepsilon}. \tag{6}$$

The relationship between the generalized stress-block parameters, α and β, and the corresponding equivalent rectangular stress-block parameters, α_1 and β_1, can be developed through geometry and equating the resulting compressive force, C, from the two stress blocks in Figure 7.[25] The relationships are shown in eqs. (7) and (8).

$$\alpha_1 = \frac{\alpha}{\beta_1}, \tag{7}$$

$$\beta_1 = 2\beta \tag{8}$$

where, α and β are the generalized stress intensity coefficient and the resultant location coefficient for a generalized stress block, respectively.

Table V lists the test results and computed parameters for four sets of C-shaped specimens with different length. Each set is composed of three specimens to be averaged. In the table, P_u stands for the sum of main and subsidiary loads ($P_1 + P_2$).

Figure 8 depicts the variation of β_1 versus the ratio of length to depth r (=h/d) for the C-shaped specimens of cement concrete obtained by Yi et al.[10] and of polymer concrete surveyed in this study.

TABLE V
Test Results for C-Shape Specimens

r	P_u (kN)	ε_u ($\times 10^{-3}$)	α	β_1	α_1
1	997.2	7.84	0.69	0.83	0.84
	1009.1	7.95	0.69	0.81	0.85
	1011.9	7.98	0.69	0.82	0.84
2	921.3	8.02	0.65	0.76	0.85
	912.9	8.10	0.65	0.76	0.86
	900.3	8.08	0.63	0.73	0.86
3	882.5	8.08	0.62	0.74	0.84
	874.2	7.98	0.62	0.74	0.84
	872.0	7.89	0.62	0.72	0.86
4	884.5	7.88	0.62	0.72	0.86
	874.5	7.96	0.62	0.74	0.83
	866.5	8.03	0.61	0.71	0.86
Average	917.2	7.98	0.64	0.76	0.85

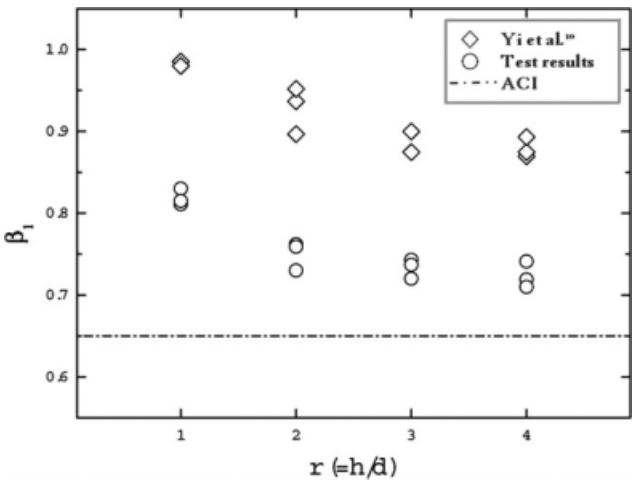

Figure 8 Depth of the equivalent rectangular stress block versus ratio of length to depth.

Horizontal dashed line represents the constant value of 0.65 suggested by ACI 318 Code[26] for the rectangular stress block width of $0.85f'_c$ with $f'_c \geq 56$ MPa. In this study, f'_c for the cylinder specimen of polymer concrete is about 100 MPa, and despite that β_1 values decrease gradually as the ratio of length to depth increases for polymer concrete, these are larger than the values suggested by ACI (Fig. 8) and smaller than the values surveyed for cement concrete by Yi et al.[10] That is because that polymer concretes using UP resin as a binder has smaller elastic modulus and much larger plastic region than the high-strength cement concretes do. ACI 318 Code regulates α_1 as 0.85 regardless of the strength of concretes. In this study, the values α_1 of polymer concretes were about 0.85 regardless of the specimen lengths. In Table VI, three different cases of the stress-block parameters are compared.

Length effect on flexural compressive strength

Yi et al.[10] proposed a modified size effect law by introducing the size independent strength $\sigma_0(=\chi f'_t)$ for the case of real concrete specimens without initial cracks or with dissimilar initial cracks as eq. (7).

$$\sigma_N = \frac{Bf'_t}{\sqrt{1 + d_c/(\lambda_0 d_a)}} + \chi f'_t, \tag{7}$$

where, σ_N is nominal strength, f'_t is direct tensile strength of cylinder specimen, d_c is characteristic dimension, and d_a is maximum aggregate size. Parameters of B, λ_0, and χ (<1) are empirical constants. For applying the equation, they reported the experimental results for cylinder specimens subjected to compressive load and for C-shaped specimens subjected to flexural compressive load.

For concrete cylinder specimen, Markeset[27] and Markeset and Hillerborg[28] reported experimental results that showed the postpeak energy per unit area is independent of the specimen length when the slenderness ratio is greater than 2.50. Jansen and Shah[29] also reported experimental results in which prepeak energy per unit cross-sectional area increases proportionally with specimen length and postpeak energy per unit cross-sectional area does not change with specimen length if the lengths are larger than 20 cm in concrete cylinders. Yi et al.[10] showed that flexural compressive strength does not change for specimens having a length larger than 30 cm for C-shaped reinforced concrete specimens.

To obtain an analytical model that can predict the flexural compressive strength of C-shaped polymer concrete specimens at failure, in this study, eq. (7) is used as the basic equation for the regression analyses of the experimental results of length effect. The predicted length effect equation is given as eq. (8)

$$\sigma_N(r) = \frac{Bf'_c}{\sqrt{1 + P\,r}} + \chi f'_c, \tag{8}$$

where B, P, and χ are empirical constants. Three specimens per each specimen length were tested and regression analyses were carried out to obtain eq. (9) as follows:

$$\begin{cases} \sigma_N(r) = \dfrac{2.59f'_c}{\sqrt{1 + 110.9\,r}} + 0.56f'_c \quad (r \leq 3.0) \\ \sigma_N(r) = 0.7f'_c \quad (r > 3.0) \end{cases}, \tag{9}$$

where, $\sigma_N(r)$ is flexural compressive strength and f'_c is the compressive strength of cylinder specimens in the unit of N/m^2.

Experimental results are plotted as shown in Figure 9. Figure 9 indicates strong length-dependent size effect of polymer concrete specimens. For r less than 3.0, the flexural compressive strength decreases with increasing length of the specimen; whereas for r greater than 3.0, it converges to a constant value of $0.7f'_c$. From these test results, we can conclude that flexural compressive strength does not change for specimens having a length greater than 30 cm for C-shaped polymer concrete specimens. Because that the ratio of length to depth (r) of normal flexural members is greater than 3.0, we also conclude that

TABLE VI
Comparison of Stress Block Parameters

Description	α	β_1	α_1
Cement concrete ($f'_c \geq 55$ MPa)[25]	0.56	0.65	0.86
Cement concrete ($f'_c \approx 58$ MPa, average)[10]	0.71	0.83	0.85
Polymer concrete ($f'_c \approx 100$ MPa, average)	0.64	0.76	0.85

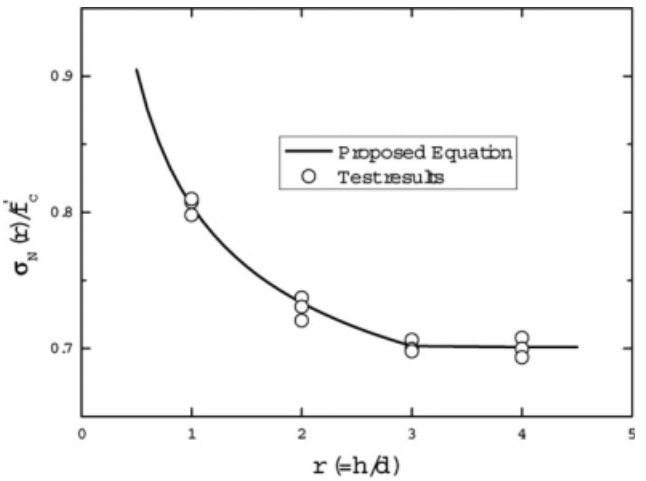

Figure 9 Normalized nominal strength with compressive strength versus ratio of length to depth.

the flexural compressive strength of polymer concrete flexural members can be reasonably set as $0.7f'_c$.

CONCLUSIONS

From studies for stress–strain relation, stress-block parameters, and length effect of compressive strength of polymer concrete, the following conclusions are drawn.

The stress–strain relation of single curve for the C-shaped polymer concrete structures was proposed. Formulating the new model, we took account the average slope of descending branch beyond the peak stress point. The proposed model well agrees with the test results for the specimens of four different ratios of length to depth.

The analytical stress–strain relation was numerically integrated to compute the rectangular stress-block parameters. The parameters of β_1 were greater than the values regulated in ACI 318 Code for cement concrete and regardless of the lengths of specimens, α_1 was about 0.85, which is similar to the existing test results for cement concretes. That is because the polymer concretes using UP resin as a binder have smaller elastic modulus and much larger plastic region than the high-strength cement concretes have.

Test results indicate that polymer concretes have strong length-dependent size effect. For r less than 3.0, the flexural compressive strength decreases with increasing length of the specimen; whereas for r greater than 3.0, it converges to a constant value of $0.7f'_c$. It can be concluded that flexural compressive strength does not change for specimens having a length greater than 30 cm for C-shaped polymer concrete specimens, and that it can be reasonably set as $0.7f'_c$.

References

1. Helal, M. S. Experimental Study of Mechanical Properties and Structural Applications of Polymer Concrete, Ph.D. Dissertation; University of Rice, Houston, 1978.
2. Knab, L. I.; Cook, J. P. J Am Concr Inst 1974, 71, 493.
3. Knab, L. I. Flexural Behavior of Conventionally Reinforced Polyester Concrete Beams, Ph.D. Dissertation; University of Cincinnati, Cincinnati, 1972.
4. Lott, J.; Naus, D.; Howdyshell, P. Am Concr Inst SP 1973, 40, 295.
5. Vipulanandan, C.; Dharmarajan, N.; Chingn, E. Mater Struct 1988, 21, 268.
6. Ribeiro, M. C. S.; Tavares, C. M. L.; Figueiredo, M.; Ferreira, A. J. M.; Fernandes, A. A. Mater Res 2003, 6, 247.
7. Vipulanandan, C.; Paul, E. Mechanical properties of epoxy and polyester polymers and polymer concrete systems, Report No. UHCE 88-13, Houston, 1988.
8. Kim, J. K.; Yi, S. T. Sādhāna 2002, 27, 467.
9. JIS A 1181. Test Methods for Polymer Concrete; Japanese Industrial Standard: Tokyo, 2005.
10. Yi, S. T.; Lee, M. S.; Kim, J. K.; Kim, J. J. H. Cement Concr Compos 2007, 29, 230.
11. Hognestad, E.; Hanson, N. W.; McHenry, D. Am Concr Inst Struct J 1955, 52, 455.
12. Kent, D. C.; Park, R. J Struct Div 1971, 97, 1969.
13. Sheikh, S. A.; Uzumeri, S. M. J Struct Div 1982, 108, 2703.
14. Roy, H. E. H.; Sozen, M. A. In Proceedings of the International Symposium on Flexural Mechanics of R.C.; ASCE-ACI Joint Symposium: Miami, 1964, p 213.
15. Sargin, M. Stress–strain relationships for concrete and the analysis of structural concrete section, Ph.D. Dissertation; University of Waterloo, Ontario, Canada, 1971.
16. Saatcioglu, M.; Razvi, S. R. J Struct Eng 1992, 118, 590.
17. Muguruma, H.; Nishiama, M.; Watanabe, F. In Proceedings of Symposium on Utilization of High Strength Concrete; Holand, I., Sellevold, E., Eds.; Lillehammer, Norway, 1993; Vol. 1, p 314.
18. Collins, M. P.; Mitchell, D.; MacGregor, J. G. Concr Int Des Constr 1993, 15, 27.
19. Hsu, L. S.; Hsu, C. T. Mag Concr Res 1994, 46, 301.
20. Sargin, M.; Handa, V. K. In Structural Concrete and Some Numerical Solutions; Proceedings of the 23rd ACM National Conference: New York, 1968; p 563.
21. Ahmad, S. H.; Shah, S. P. J Am Concr Inst 1982, 79, 484.
22. Sun, O. P.; Sakino, G. Annu Rep Concr Eng 1993, 15, 719.
23. Saenz, L. P. J Am Concr Inst 1964, 61, 1229.
24. Whitney, C. S. Am Concr Inst Struct J 1937, 33, 483.
25. Urgessa, G.; Horton, S.; Reda Taha, M. M.; Maji, A. ACI Spec Publ 2005, 230, 1531.
26. ACI Committee 318-89. Building Code Requirements for Reinforced Concrete; American Concrete Institute: Detroit, 2008.
27. Markeset, G. A. Compressive Softening Model for Concrete: Fracture Mechanics of Concrete Structures; Wittmann, F. H., Ed.; FRAMCOS-2, AEDIFICATIO Publishers: Freiburg, Germany, 1995; p 435.
28. Markeset, G. A.; Hillerborg, A. Cement Concr Res 1995, 25, 702.
29. Jansen, D. C.; Shah, S. P. J Eng Mech 1997, 123, 251.